Temperature dependence of the side-jump spin Hall conductivity

Cong Xiao,[1] Yi Liu,[2] Zhe Yuan,[2,*] Shengyuan A. Yang,[3] and Qian Niu[1]
[1]*Department of Physics, The University of Texas at Austin, Austin, Texas 78712, USA*
[2]*The Center for Advanced Quantum Studies and Department of Physics, Beijing Normal University, 100875 Beijing, China*
[3]*Research Laboratory for Quantum Materials, Singapore University of Technology and Design, Singapore 487372, Singapore*

(Received 25 September 2018; revised manuscript received 3 July 2019; published 16 August 2019)

In the conventional paradigm of the spin Hall effect, the side-jump conductivity due to electron-phonon scattering is regarded to be temperature independent. In contrast, we draw the distinction that, while this side-jump conductivity is temperature independent in the classical equipartition regime where the longitudinal resistivity is linear in temperature, it can be temperature dependent below the equipartition regime. The mechanism resulting in this temperature dependence differs from the familiar one of the longitudinal resistivity. In the concrete example of Pt, we show that the change of the spin Hall conductivity with temperature can be as high as 50%. Experimentally accessible high-purity Pt is proposed to be suitable for observing this prominent variation below 80 K.

DOI: 10.1103/PhysRevB.100.085425

I. INTRODUCTION

The spin Hall effect refers to a transverse spin current in response to an external electric field [1]. In strongly spin-orbit-coupled electronic systems such as 4d and 5d transition metals [2–10] and Weyl semimetals [11], the spin Hall conductivity due solely to the geometry of Bloch bands, the so-called spin Berry curvature, has attracted much attention. Additionally, there is a scattering-induced mechanism called the side jump, the contribution of which to the spin Hall conductivity turns out to be of zeroth order of scattering time and independent of the density of a given type of impurities [1]. Furthermore, the side-jump spin Hall conductivity arising from the electron-phonon scattering is conventionally regarded to be temperature (T) independent although the phonon density varies with T [12,13].

In this paper we draw the distinction that, while the electron-phonon scattering-induced side-jump spin Hall conductivity is T independent in the classical equipartition regime where the longitudinal resistivity ρ is linear in T, it can be T dependent at temperatures below the equipartition regime in strongly spin-orbit-coupled systems. This character distinguishes the side jump from the geometric contribution, and provides a mechanism for T-dependent spin Hall conductivities in high-purity experimental samples. An intuitive picture is proposed for the T dependence of the side-jump conductivity, which differs from ρ, which is always T dependent. Moreover, our first-principles calculation demonstrates a prominent T variation of the spin Hall conductivity in experimentally accessible high-purity Pt below 80 K.

We consider strongly spin-orbit-coupled multiband systems. The Fermi energy and the interband splitting around the Fermi level are assumed to be much larger than room temperature, thus the thermal smearing of the Fermi surface is negligible. Aiming to provide semiquantitative and intuitive understanding, the electron-phonon scattering is approximated by a single-electron elastic process, which can be called the "quasi-static approximation." In calculating the resistivity resulting from phonon scattering, this approximation produces not only the correct low-T power law ($\rho \sim T^5$ for three-dimensional isotropic single-Fermi-surface systems) [14] but also the values that are quantitatively comparable with experimental data [15]. When applied to the side-jump transport, the high-T and low-T asymptotic behaviors are grasped in this approximation. Quantitative deviations appearing in the intermediate temperature regime are not essential for the present purpose.

The side jumps were originally proposed as the sideways shifts in opposite transverse directions of carriers with different spins, when they are scattered by spin-orbit active impurities [12,16]. This picture works well in systems with weak spin-orbit coupling [17–19], where the spin-orbit-induced band splitting is smeared by disorder broadening [1], whereas in strongly spin-orbit-coupled Bloch bands of current interest the side-jump contribution arises microscopically from the scattering-induced band-off-diagonal elements of the out-of-equilibrium density matrix [20–23]. This corresponds, in the Boltzmann transport formalism, to the dressing of Bloch states by interband virtual scattering processes involving off-shell states away from the Fermi surface [24].

Our paper is organized as follows. In Sec. II we present the theory for the side-jump spin Hall effect, emphasizing the indispensable role played by off-shell Bloch states. In Sec. III, the T dependence of the phonon-induced side-jump spin Hall conductivity is analyzed, including the general argument and an intuitive physical picture. This T dependence is supported by the first-principles calculations in pure Pt in Sec. IV, where a T variation of the spin Hall conductivity up to 50% is found. Experimentally accessible high-purity Pt is proposed to be a compelling candidate to observe the predicted phenomenon. Finally, in Sec. V, we conclude this paper.

*zyuan@bnu.edu.cn

II. TRANSPORT FORMALISM INVOLVING OFF-SHELL STATES

In weakly disordered crystals perturbed by a weak external electric field $\mathbf{E}$, the expectation value of an observable $\mathbf{A}$ (assumed to be a vector without loss of generality) reads

$$\langle \mathbf{A} \rangle = \sum_l \mathbf{A}_l f_l \tag{1}$$

in the Boltzmann transport formalism, where f_l is the occupation function of the carrier state marked by $l = (\eta, \mathbf{k})$ with η the band index and $\mathbf{k}$ the crystal momentum, and $\mathbf{A}_l$ is the quantum-mechanical average on state l. The carrier state is the Bloch state dressed by interband virtual processes induced by both the electric field and the scattering [24]. In the linear-response and weak scattering regime, these two dressing effects are independent [24]:

$$\mathbf{A}_l = \mathbf{A}_l^0 + \mathbf{A}_l^{\mathrm{bc}} + \mathbf{A}_l^{\mathrm{SJ}}, \tag{2}$$

where

$$\left(\mathbf{A}_l^{\mathrm{bc}}\right)_\beta = \frac{e}{\hbar} \mathbf{E}_\alpha \Omega^A_{\alpha\beta}(\eta\mathbf{k}) \tag{3}$$

arises from the electric-field induced dressing, with

$$\Omega^A_{\alpha\beta}(\eta\mathbf{k}) = -2\hbar^2 \,\mathrm{Im} \sum_{\eta'' \neq \eta} \frac{v_\alpha^{\eta\eta''}(\mathbf{k}) A_\beta^{\eta''\eta}(\mathbf{k})}{(\epsilon_{\eta\mathbf{k}} - \epsilon_{\eta''\mathbf{k}})^2}, \tag{4}$$

and

$$\begin{aligned}\left(\mathbf{A}_l^{\mathrm{SJ}}\right)_\beta = & -2\pi \sum_{\eta'\mathbf{k}'} W_{\mathbf{k}\mathbf{k}'} \delta(\epsilon_{\eta\mathbf{k}} - \epsilon_{\eta'\mathbf{k}'}) \\ & \times \mathrm{Im} \left[\sum_{\eta'' \neq \eta'} \frac{\langle u_{\eta\mathbf{k}} | u_{\eta'\mathbf{k}'} \rangle \langle u_{\eta''\mathbf{k}'} | u_{\eta\mathbf{k}} \rangle A_\beta^{\eta'\eta''}(\mathbf{k}')}{\epsilon_{\eta'\mathbf{k}'} - \epsilon_{\eta''\mathbf{k}'}} \right. \\ & \left. - \sum_{\eta'' \neq \eta} \frac{\langle u_{\eta''\mathbf{k}} | u_{\eta'\mathbf{k}'} \rangle \langle u_{\eta'\mathbf{k}'} | u_{\eta\mathbf{k}} \rangle A_\beta^{\eta\eta''}(\mathbf{k})}{\epsilon_{\eta\mathbf{k}} - \epsilon_{\eta''\mathbf{k}}} \right]\end{aligned} \tag{5}$$

originates from the scattering-induced dressing. Equation (5) is diagrammatically represented in Fig. 1. The summation over repeated spatial indices α and β is implied hereafter. Here $A_\beta^{\eta''\eta}(\mathbf{k}) \equiv \langle u_{\eta''\mathbf{k}} | A_\beta | u_{\eta\mathbf{k}} \rangle$ with $|u_{\eta\mathbf{k}}\rangle$ the periodic part of the Bloch state. For impurities, $W_{\mathbf{k}\mathbf{k}'} = n_i |V^o_{\mathbf{k}\mathbf{k}'}|^2$, with n_i the impurity density and $V^o_{\mathbf{k}\mathbf{k}'}$ the plane-wave part of the matrix element of the impurity potential. For electron-phonon scattering,

$$W_{\mathbf{k}\mathbf{k}'} = \frac{2N_\mathbf{q}}{V} \left| U^o_{\mathbf{k}\mathbf{k}'} \right|^2, \tag{6}$$

where $U^o_{\mathbf{k}'\mathbf{k}}$ is the plane-wave part of the electron-phonon matrix element, $N_\mathbf{q}$ is the Bose occupation function of phonons ($\mathbf{q}$ is the wave vector of phonons with energy $\hbar\omega_q$), V is the volume (area in two dimensions) of the system, and the factor 2 accounts for the absorption and emission of phonons.

When calculating the electric current $\mathbf{A} = e\mathbf{v}$, $\Omega^A_{\alpha\beta}$ and $\mathbf{v}_l^{\mathrm{SJ}}$ are the Berry curvature and "side-jump velocity" [22,24,25], respectively. When calculating the spin current $\mathbf{A} = \mathbf{j}$, $\Omega^A_{\alpha\beta}$ is the so-called spin Berry curvature [11], whereas $\mathbf{A}_l^{\mathrm{SJ}}$ provides the spin-current counterpart of the side-jump velocity [24,26].

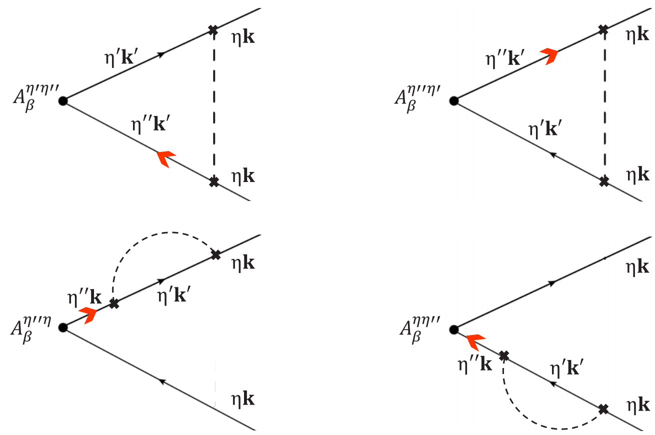

FIG. 1. Graphical representation of Eq. (5), where the off-shell states away from the Fermi surface are marked by red arrows. $W_{\mathbf{k}\mathbf{k}'}$ is represented by the disorder line connected with two interaction vertices.

The occupation function of the carrier states is decomposed, around the Fermi distribution f_l^0, into $f_l = f_l^0 + g_l^{2s} + g_l^a$. Its out-of-equilibrium part satisfies the linearized steady-state Boltzmann equations $e\mathbf{E} \cdot \mathbf{v}_l^0 \partial f_l^0 / \partial \epsilon_l = -\sum_{l'} w^{2s}_{ll'} (g_l^{2s} - g_{l'}^{2s})$ and

$$e\mathbf{E} \cdot \mathbf{v}_l^{\mathrm{SJ}} \partial f_l^0 / \partial \epsilon_l = \sum_{l'} w^{2s}_{ll'} \left(g_l^a - g_{l'}^a \right) \tag{7}$$

in the presence of weak scalar disorder [22]. $w^{2s}_{ll'} = \frac{2\pi}{\hbar} W_{\mathbf{k}\mathbf{k}'} |\langle u_l | u_{l'} \rangle|^2 \delta(\epsilon_l - \epsilon_{l'})$ is the lowest-Born-order scattering rate, and $\mathbf{v}_l^0$ is the usual band velocity.

Collecting the above ingredients, the spin Hall current is $j_{\mathrm{SH}} = j^{\mathrm{bc}}_{\mathrm{SH}} + j^{\mathrm{SJ}}_{\mathrm{SH}} + j^{\mathrm{ad}}_{\mathrm{SH}}$. The first two terms,

$$j^{\mathrm{bc}}_{\mathrm{SH}} = \sum_l \left(j_l^{\mathrm{bc}} \right) f_l^0, \quad j^{\mathrm{SJ}}_{\mathrm{SH}} = \sum_l \left(j_l^{\mathrm{SJ}} \right) g_l^{2s}, \tag{8}$$

arise from off-shell-state induced corrections to the semiclassical value of j_l^0, whereas $j^{\mathrm{ad}}_{\mathrm{SH}} = \sum_l j_l^0 g_l^a$ incorporates the nonequilibrium occupation function modified by off-shell states, since g_l^a appears as a response to the generation term proportional to the side-jump velocity $\mathbf{v}_l^{\mathrm{SJ}}$ [25]. In calculating the anomalous Hall (AH) current [21] $\mathbf{A} = e\mathbf{v}$, $j^{\mathrm{SJ}}_{\mathrm{AH}}$ and $j^{\mathrm{ad}}_{\mathrm{AH}}$ are related to the transverse (sideways) and longitudinal components of $\mathbf{v}_l^{\mathrm{SJ}}$, respectively [25]. Thereby their sum is also often referred to as the side-jump contribution in the literature on the anomalous Hall effect [21,22,25]. Given this convention, we also include the $j^{\mathrm{ad}}_{\mathrm{SH}}$ contribution, although $j^{\mathrm{ad}}_{\mathrm{AH}}$ has nothing to do with the original concept of side jump, and the microscopic theory [20,23] indeed shows that g_l^a is not related to the interband elements of the out-of-equilibrium density matrix. In fact, in two-dimensional nonmagnetic models for the spin Hall effect, such as the two-dimensional electronic systems with Rashba, cubic Rashba, and Dresselhaus spin-orbit couplings [27–32], the spin current operator (for the out-of-plane spin component) has only interband matrix elements, i.e., $j_l^0 = 0$, thus $j^{\mathrm{ad}}_{\mathrm{SH}}$ does not appear at all.

III. PHONON-INDUCED T DEPENDENCE OF SPIN HALL CONDUCTIVITY

In order to show the T dependence of the phonon-induced side-jump spin Hall conductivity, we first prove that its values in the low-T and high-T limits can be different.

In the low-T limit, $W_{\mathbf{kk}'}$ for phonon scattering is highly peaked at the vanishing scattering angle, and the on-shell scattering can only be the intraband transition, hence in Eq. (5) $\eta' = \eta$ and $\mathbf{k}'$ is very close to $\mathbf{k}$. We then expand the integrand up to the first order of $(\mathbf{k}' - \mathbf{k})$, getting $(\mathbf{A}_l^{\mathrm{SJ}})_\beta = \sum_{\mathbf{k}'} \tilde{\omega}_{l'l}^{2s} \Omega_{\alpha\beta}^A(\eta\mathbf{k})(\mathbf{k}' - \mathbf{k})_\alpha$, with $\tilde{\omega}_{l'l}^{2s} = \frac{2\pi}{\hbar} W_{\mathbf{kk}'} \delta(\epsilon_{\eta\mathbf{k}} - \epsilon_{\eta\mathbf{k}'})$ the scattering rate in the small-scattering-angle limit. Concurrently, $\mathbf{v}_l^{\mathrm{SJ}} = \sum_{\mathbf{k}'} \tilde{\omega}_{l'l}^{2s} \mathbf{\Omega}(l) \times (\mathbf{k}' - \mathbf{k})$ ($\mathbf{\Omega}$ is the vector form of the ordinary Berry curvature) yields $g_l^a = e\mathbf{E} \cdot [\mathbf{k} \times \mathbf{\Omega}(l)] \partial f_l^0 / \partial \epsilon_l$. Thus one has

$$\left(j_{\mathrm{SH}}^{\mathrm{SJ}}\right)_\beta = e \sum_l \mathbf{k}_\alpha \Omega_{\alpha\beta}^j(l) \mathbf{E} \cdot \mathbf{v}_l^0 \partial f_l^0 / \partial \epsilon_l \tag{9}$$

and

$$\left(j_{\mathrm{SH}}^{\mathrm{ad}}\right)_\beta = e \sum_l \left(j_l^0\right)_\beta \mathbf{E} \cdot [\mathbf{k} \times \mathbf{\Omega}(l)] \partial f_l^0 / \partial \epsilon_l. \tag{10}$$

Thus $\sigma_{\mathrm{SH}} = (j_{\mathrm{SH}})_x / E_y$ is a T-independent constant in the low-T limit. It is clear that this constant equals that contributed by scalar impurities in the long-range limit, the $W_{\mathbf{kk}'}$ of which is also highly concentrated around the vanishing scattering angle.

In the high-T limit, the phonon energy is much smaller than $k_B T$, indicating $W_{\mathbf{kk}'} = 2k_B T \mathrm{V}^{-1} |U_{\mathbf{k}'\mathbf{k}}^o|^2 / \hbar\omega_q$; then we have $g_l^{2s} \sim T^{-1}$, $j_l^{\mathrm{SJ}} \sim T$, and $g_l^a \sim T^0$, and, consequently,

$$\rho \sim T, \quad \sigma_{\mathrm{SH}} \sim T^0. \tag{11}$$

Accordingly, in practice the high-T limit is identified as the equipartition regime with linear-in-T resistivity [14]. This regime is usually marked qualitatively by $T > T_D$ in textbooks, with T_D the Debye temperature, but can extend practically to about $T > T_D/3$ in Pt, Cu, and Au [15,33], and to about $T > T_D/5$ in Al [33]. Additionally, it is apparent that the T-independent σ_{SH} in the equipartition regime can be different from that in the low-T limit.

To acquire a more transparent picture, we assume any large-angle electron-phonon scattering can occur via normal processes, and we take the approximation of the deformation-potential electron-acoustic phonon coupling, for which an electron-phonon coupling constant can be introduced as [34,35] $\lambda^2 = 2\mathrm{V}^{-1} |U_{\mathbf{k}'\mathbf{k}}^o|^2 / \hbar\omega_q$, hence we arrive at $W_{\mathbf{kk}'} = \lambda^2 k_B T$ in the high-T regime. This $W_{\mathbf{kk}'}$ is uniformly distributed on the Fermi surface, similar to $W_{\mathbf{kk}'} = n_i V_i^2$ contributed by randomly distributed zero-range scalar impurities, with V_i the strength. Therefore, we infer that the σ_{SH} due to phonons in the high-T equipartition regime takes the same value as that due to zero-range scalar impurities. This speculation can be verified by noticing that $g_l^{2s,ep} \lambda^2 k_B T = g_l^{2s,ei} n_i V_i^2$, $(\mathbf{A}_l^{\mathrm{SJ}})^{ep} / \lambda^2 k_B T = (\mathbf{A}_l^{\mathrm{SJ}})^{ei} / n_i V_i^2$, and $g_l^{a,ep} = g_l^{a,ei}$, where the superscripts "ep" and "ei" mean the contributions due to electron-phonon scattering and zero-range scalar impurities, respectively.

According to the above results, σ_{SH} induced by electron-acoustic phonon scattering is T dependent provided that the σ_{SH} values induced by scalar impurity scattering in the long-range and zero-range limits are different. This unexpected relation in turn provides a qualitative picture for comprehending the T dependence of the phonon-induced side jump, by analogy with the recently revealed sensitivity of the side-jump conductivity to the scattering range of impurities [36]. The accessible phase space of the electron-phonon scattering changes with temperature, thus implying a T-dependent average momentum transfer, i.e., effective range, of this scattering.

Note that this mechanism differs from that for the T-dependent ρ. To directly see this point, one need only consider the fact that in the equipartition regime $\sigma_{\mathrm{SH}} \sim T^0$ although $\rho \sim T$ is still T dependent.

The above revealed relation facilitates judging whether a model system has a T-dependent phonon-induced side-jump conductivity based on the familiar knowledge about the impurity-induced side jump. There are models which possess different side-jump conductivities induced by scalar impurity-scattering in the long-range and zero-range limits, such as the Luttinger model describing p-type semiconductors [37] and the k-cubic Rashba model for two-dimensional heavy-hole gas in confined quantum wells [28]. In these systems the phonon-induced side-jump conductivities are thus T dependent.

In the k-cubic Rashba model [31,32], the Hamiltonian reads

$$\hat{H} = \frac{\hbar^2 \mathbf{k}^2}{2m} + i\frac{\alpha_R}{2}(\hat{\sigma}_+ k_-^3 - \hat{\sigma}_- k_+^3), \tag{12}$$

where $\mathbf{k} = k(\cos\phi, \sin\phi)$ is the two-dimensional wave vector, $k_\pm = k_x \pm ik_y$, $\hat{\sigma}$'s are Pauli matrices with $\hat{\sigma}_\pm = \hat{\sigma}_x \pm i\hat{\sigma}_y$, and α_R is the spin-orbit coupling coefficient that can be tuned to very large values by the gate voltage [32]. The spin current operator [29,30] $\hat{j}_x = \frac{3\hbar}{2}\frac{1}{2}\{\hat{\sigma}_z, \hat{v}_x\}$ has only interband components, hence $j_{\mathrm{SH}} = j_{\mathrm{SH}}^{\mathrm{bc}} + j_{\mathrm{SH}}^{\mathrm{SJ}}$. Letting $\eta = \pm$ label the two Rashba bands, the spin Berry curvature is $\Omega_{yx}^j(\eta\mathbf{k}) = -\eta\frac{9\hbar^3 \sin^2\phi}{4m\alpha_R k^3}$, thus $\sigma_{\mathrm{SH}}^{\mathrm{bc}} = (j_{\mathrm{SH}}^{\mathrm{bc}})_x / E_y = \frac{9e\hbar^2}{16\pi m\alpha_R} \sum_\eta \eta k_\eta^{-1}$ [28,29], with k_η the Fermi wave number of band η. The side-jump spin Hall conductivity due to electron-phonon scattering in the low-T limit is given by Eq. (9) as

$$\sigma_{\mathrm{SH}}^{\mathrm{SJ}} = \left(j_{\mathrm{SH}}^{\mathrm{SJ}}\right)_x / E_y = \frac{1}{4}\sigma_{\mathrm{SH}}^{\mathrm{bc}}. \tag{13}$$

When $m\alpha_R/\hbar^2 \ll 1/\sqrt{\pi n}$ [29], one has $\sigma_{\mathrm{SH}}^{\mathrm{SJ}} = 9e/32\pi$. In the high-$T$ regime, we have $j_l^{\mathrm{SJ}} = 0$, leading to

$$\sigma_{\mathrm{SH}}^{\mathrm{SJ}} = 0. \tag{14}$$

Since the side-jump conductivities in the high-T and low-T limits are different, there must be a crossover in the intermediate regime resulting in the T-dependent behavior.

IV. TEMPERATURE-DEPENDENT SPIN HALL CONDUCTIVITY IN PURE PLATINUM

To show the applicability of our theoretical ideas in real materials, we perform a first-principles calculation to the spin

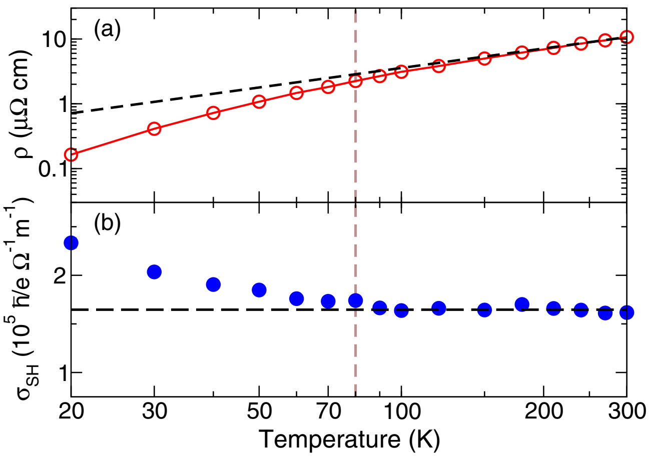

FIG. 2. Calculated longitudinal resistivity ρ (a) and spin Hall conductivity σ_{SH} (b) of pure Pt as a function of temperature. The black dashed line in panel (a) illustrates the linear dependence.

Hall conductivity of pure Pt in the range 20–300 K. The minimal interband splitting around the Fermi level of Pt is much larger than 300 K [9], thus the spin Berry-curvature contribution should be T independent up to 300 K. The temperature is modeled by populating the calculated phonon spectra of Pt into a large supercell with its length L along fcc [111] and 5×5 unit cells in the lateral dimensions [15,38]. Then the transport calculation is carried out using the above disordered (finite-temperature) supercell sandwiched by two perfectly crystalline (zero-temperature) Pt electrodes. The scattering matrix is obtained using the so-called wave-function matching technique within the Landauer-Büttiker formalism [38]. The calculated total resistance of the scattering geometry is found to be linearly dependent on L following Ohm's law. By varying L in the range of 5–60 nm, we extract the resistivity at every temperature using a linear least-squares fitting for the calculated resistances. For each L, at least ten random configurations have been considered to ensure both average value and standard deviation well converged with respect to the number of configurations. The calculated resistivity ρ is plotted in Fig. 2(a) as a function of temperature. The spin-Hall angle Θ_{SH} is computed by examining the ratio of transverse spin current density and longitudinal charge current density [10]. At every temperature, we use more than 20 random configurations, each of which contains 60-nm-long disordered Pt. Then the spin Hall conductivity is obtained as $\sigma_{SH} = (\hbar/e)\Theta_{SH}/\rho$, shown in Fig. 2(b).

For $T \gtrsim 80$ K, a linear-in-T ρ is obtained, and σ_{SH} is approximately a constant of $1.6 \times 10^5 \hbar/e(\Omega\,\mathrm{m})^{-1}$ [10]. Below the equipartition regime, ρ deviates from the linear T dependence [illustrated by the black dashed line in Fig. 2(a)], and concurrently the calculated σ_{SH} increases with decreasing temperature. At $T = 20$ K, σ_{SH} reaches $2.3 \times 10^5 \hbar/e(\Omega\,\mathrm{m})^{-1}$. Compared to the value at 80 K, the T variation of σ_{SH} is as large as 50%. This T dependence begins when the temperature drops below the equipartition regime, in agreement with our theoretical prediction.

Finally, we discuss the possibility of observing the predicted effect in experiments. In high-purity metals, the electron-electron scattering dominates over the electron-phonon scattering in determining transport behaviors at very low temperature. To observe our prediction, lower characteristic temperature T_t marking the crossover from the electron-electron dominated regime to the electron-phonon dominated one is required, such that the intermediate range from T_t to the high-T equipartition regime is wide enough. In experimentally accessible high-purity Pt samples with residual resistivity as small as 10^{-3}-10^{-2} $\mu\Omega$ cm [39,40], T_t can be as low as 10 K, and at $T = 20$ K the phonon-induced ρ is nearly one order of magnitude larger than that contributed by the electron-electron scattering and the residual resistivity [40]. Because in high-purity Pt the T-linear scaling of ρ emerges at $T \gtrsim 80$ K [15], the suitable range for observing the first-principles predicted T dependence of σ_{SH} [Fig. 2(b)] is $20 \lesssim T \lesssim 80$ K. Very recently experimentalists have been developing new techniques, with which the spin current is generated and detected in a single transition-metal sample, thus avoiding all the complications associated with the interfaces and shunting effect [7,8]. The predicted effect is expected to be observed as the quality of Pt samples in such measurements is improved.

V. SUMMARY

In summary, we have drawn the distinction that the side-jump spin Hall conductivity, while T independent in the classical equipartition regime where the longitudinal resistivity is linear in T, is T dependent below the equipartition regime. This contradicts the conventional belief that the side-jump conductivity due to electron-phonon scattering is T independent. The mechanism resulting in this T dependence differs from that of the longitudinal resistivity, which is always T dependent. Our theoretical idea gains support from first-principles calculations in Pt, for which the T variation of the spin Hall conductivity below the equipartition regime is found to be as high as 50%. Experimentally accessible high-purity Pt is argued to be suitable for observing this prominent variation below 80 K.

ACKNOWLEDGMENTS

We thank T. Chai, M. Xie, and H. Liu for helpful discussions. Q.N. is supported by the U.S. Department of Energy (Grant No. DE-FG03-02ER45958, Division of Materials Science and Engineering) on the transport formulation in this work. C.X. is supported by NSF (Grant No. EFMA-1641101) and Welch Foundation (Grant No. F-1255). S.A.Y. is supported by Singapore Ministry of Education AcRF Tier 2 (Grant No. MOE2017-T2-2-108). Y.L. and Z.Y. are supported by the National Natural Science Foundation of China (Grants No. 61604013, No. 61774018, and No. 11734004), the Recruitment Program of Global Youth Experts, and the Fundamental Research Funds for the Central Universities (Grants No. 2016NT10 and No. 2018EYT03).

[1] J. Sinova, S. O. Valenzuela, J. Wunderlich, C. H. Back, and T. Jungwirth, Rev. Mod. Phys. **87**, 1213 (2015).
[2] A. Hoffmann, IEEE Trans. Magn. **49**, 5172 (2013).
[3] T. Seki, Y. Hasegawa, S. Mitani, S. Takahashi, H. Imamura, S. Maekawa, J. Nitta, and K. Takanashi, Nat. Mater. **7**, 125 (2008).
[4] O. Mosendz, J. E. Pearson, F. Y. Fradin, G. E. W. Bauer, S. D. Bader, and A. Hoffmann, Phys. Rev. Lett. **104**, 046601 (2010).
[5] L. Liu, C.-F. Pai, Y. Li, H. W. Tseng, D. C. Ralph, and R. A. Buhrman, Science **336**, 555 (2012).
[6] E. Sagasta, Y. Omori, M. Isasa, M. Gradhand, L. E. Hueso, Y. Niimi, Y. C. Otani, and F. Casanova, Phys. Rev. B **94**, 060412(R) (2016).
[7] C. Stamm, C. Murer, M. Berritta, J. Feng, M. Gabureac, P. M. Oppeneer, and P. Gambardella, Phys. Rev. Lett. **119**, 087203 (2017).
[8] C. Chen, D. Tian, H. Zhou, D. Hou, and X. Jin, Phys. Rev. Lett. **122**, 016804 (2019).
[9] T. Tanaka, H. Kontani, M. Naito, T. Naito, D. S. Hirashima, K. Yamada, and J. Inoue, Phys. Rev. B **77**, 165117 (2008).
[10] L. Wang, R. J. H. Wesselink, Y. Liu, Z. Yuan, K. Xia, and P. J. Kelly, Phys. Rev. Lett. **116**, 196602 (2016).
[11] Y. Sun, Y. Zhang, C. Felser, and B. Yan, Phys. Rev. Lett. **117**, 146403 (2016).
[12] L. Berger, Phys. Rev. B **2**, 4559 (1970).
[13] A. Crepieux and P. Bruno, Phys. Rev. B **64**, 014416 (2001).
[14] J. M. Ziman, *Principles of the Theory of Solids* (Cambridge University, Cambridge, England, 1972).
[15] Y. Liu, Z. Yuan, R. J. H. Wesselink, A. A. Starikov, M. van Schilfgaarde, and P. J. Kelly, Phys. Rev. B **91**, 220405(R) (2015).
[16] S. K. Lyo and T. Holstein, Phys. Rev. Lett. **29**, 423 (1972).
[17] H.-A. Engel, B. I. Halperin, and E. I. Rashba, Phys. Rev. Lett. **95**, 166605 (2005).
[18] W. K. Tse and S. Das Sarma, Phys. Rev. Lett. **96**, 056601 (2006).
[19] E. M. Hankiewicz and G. Vignale, Phys. Rev. B **73**, 115339 (2006).
[20] W. Kohn and J. M. Luttinger, Phys. Rev. **108**, 590 (1957); J. M. Luttinger, *ibid.* **112**, 739 (1958).
[21] N. A. Sinitsyn, J. Phys.: Condens. Matter **20**, 023201 (2008).
[22] N. A. Sinitsyn, Q. Niu, and A. H. MacDonald, Phys. Rev. B **73**, 075318 (2006).
[23] C. Xiao, Z. Z. Du, and Q. Niu, arXiv:1907.00577
[24] C. Xiao and Q. Niu, Phys. Rev. B **96**, 045428 (2017).
[25] N. A. Sinitsyn, A. H. MacDonald, T. Jungwirth, V. K. Dugaev, and J. Sinova, Phys. Rev. B **75**, 045315 (2007).
[26] C. Xiao, Front. Phys. **13**, 137202 (2018).
[27] O. V. Dimitrova, Phys. Rev. B **71**, 245327 (2005).
[28] S. Y. Liu and X. L. Lei, Phys. Rev. B **72**, 155314 (2005).
[29] J. Schliemann and D. Loss, Phys. Rev. B **71**, 085308 (2005).
[30] B. A. Bernevig and S. C. Zhang, Phys. Rev. Lett. **95**, 016801 (2005).
[31] R. Moriya, K. Sawano, Y. Hoshi, S. Masubuchi, Y. Shiraki, A. Wild, C. Neumann, G. Abstreiter, D. Bougeard, T. Koga, and T. Machida, Phys. Rev. Lett. **113**, 086601 (2014).
[32] H. Liu, E. Marcellina, A. R. Hamilton, and D. Culcer, Phys. Rev. Lett. **121**, 087701 (2018).
[33] J. M. Ziman, *Electrons and Phonons* (Clarendon, Oxford, 1960).
[34] A. A. Abrikosov, L. P. Gor'kov, and I. E. Dzyaloshinskii, *Quantum Field Theoretical Methods in Statistical Physics* (Pergamon, New York, 1965).
[35] J. Rammer and H. Smith, Rev. Mod. Phys. **58**, 323 (1986).
[36] I. A. Ado, I. A. Dmitriev, P. M. Ostrovsky, and M. Titov, Phys. Rev. B **96**, 235148 (2017).
[37] S. Murakami, Phys. Rev. B **69**, 241202(R) (2004).
[38] A. A. Starikov, Y. Liu, Z. Yuan, and P. J. Kelly, Phys. Rev. B **97**, 214415 (2018).
[39] G. K. White and S. B. Woods, Phil. Trans. R. Soc. A **251**, 273 (1958).
[40] R. H. Freeman, F. J. Blatt, and J. Bass, Phys. Kondens. Mater. **9**, 271 (1969).